Journal Name

ARTICLE

From square core to square opening: Structural diversity and magnetic properties of the oxo-bridged [$Cr^{III}Nb^{V}$] complexes

Received 00th January 20xx,
Accepted 00th January 20xx

DOI: 10.1039/x0xx00000x

www.rsc.org/

Marijana Jurić,*[a] Lidija Androš Dubraja,[a] Jasminka Popović,[a] Krešimir Molčanov,[a] Filip Torić,[b] Damir Pajić[b] and Ivor Lončarić[a]

Three heterometallic oxo-bridged compounds $[Cr_2(phen)_4(\mu\text{-}O)_4Nb_2(C_2O_4)_4]\cdot 2H_2O$ (**1**; phen = 1,10-phenanthroline), $[Cr_2(terpy)_2(H_2O)_2(\mu\text{-}O)_4Nb_2(C_2O_4)_4]\cdot 4H_2O$ (**2**; terpy = 2,2';6',2"-terpyridine) and $[Cr(terpy)(C_2O_4)(H_2O)][Cr_2(terpy)_2(C_2O_4)_2(\mu\text{-}O)_2Nb(C_2O_4)_2]\cdot 3H_2O$ (**3**) have been synthesized using a building block approach and characterized by IR spectroscopy, single-crystal and powder X-ray diffraction, magnetization measurement and DFT calculations. The molecular structures of **1** and **2**, crystallizing in $P4_22_12$ and $P2_1/n$ space groups respectively, contain square-shaped $\{Cr^{III}_2(\mu\text{-}O)_4Nb^{V}\}$ unit, while that of complex salt **3** ($P\bar{1}$ space group) consist of a mononuclear cation containing Cr^{III} and trinuclear anion in which two Cr^{III} ions are bridged by –O–Nb^{V}–O– fragment. Beside hydrogen-bonding patterns resulting in 1D- or 3D-supramolecular arrangement in **1**–**3**, an unusual intermolecular contact has been noticed between parallel oxalate moieties occurring due to electrostatic attraction of electron-rich carbonyl oxygen and severely electron-depleted carbon atom in the crystal packing of **2**. The antiferromagnetic coupling observed in all three compounds, determined from magnetization measurements (J = –13.51, –8.41 and –7.44 cm^{-1} for **1**, **2** and **3**, respectively) and confirmed by DFT calculations, originates from two Cr^{III} ions with spin 3/2 interacting through diamagnetic –O–Nb^{V}–O– bridge(s).

Introduction

Unique magnetic properties of the polynuclear complexes have been attracting attention due to their potential use for the formation of magnetic[1] and multifunctional materials.[2] A great deal of the consideration in past years has been devoted to the study of different factors influencing the nature and strength of the magnetic coupling between spins of paramagnetic metal centres connected through molecular bridges, i.e. good linkers that effectively transmit magnetic coupling [as cyanide (CN^-), azide ($N3^-$), oxalate ($C_2O_4^{2-}$), and oxo (O^{2-} or OH^-)].[3]

A facile approach for the preparation of heteropolynuclear species with predetermined structures and spin topologies, known as "complexes as ligands" or "building-block chemistry", involves the use of anionic mononuclear complexes as ligands towards a second metal ion. A building block tris(oxalato)oxoniobate(V), $[NbO(C_2O_4)_3]^{3-}$, introduced by our group, forms heterometallic complexes with different transition metal centres, through the bridging oxalate group (μ-C_2O_4),[4,5] except in the reaction with chromium(III) precursor when oxo-bridged (μ-O) complexes are formed.[6,7]

In our previous work we reported heterotetranuclear compound $[Cr_2(bpy)_4(\mu\text{-}O)_4Nb_2(C_2O_4)_4]\cdot 3H_2O$ (bpy = 2,2'-bipyridine) which crystallizes in the orthorhombic *Pcab* space group and contains a square shaped $\{Cr_2(\mu\text{-}O)_4Nb_2\}$ core, exhibiting relatively strong antiferromagnetic coupling between two chromium(III) ions (J = –12.77 cm^{-1}) mediated by two diamagnetic –O–Nb^{V}–O–bridges.[6] The occurrence of this unexpected magnetic exchange interaction between two paramagnetic metal centres [separated more than 7.4 Å by three diamagnetic atoms, one of which is a metal ion of niobium(V)] inspired us to investigate the effect of different ancillary ligands, i.e. aromatic *N*-donor ligands (as phenanthroline and terpyridine) on structural features and magnetic properties of new [$Cr^{III}Nb^{V}$] compounds. In general, complexes with exchange interactions between paramagnetic metal centres through diamagnetic metal as magnetic-communication bridge are known, but very scarce and unexplored,[7–13] and this prompted us to continue with this interesting research. Up to now, the strongest antiferromagnetic exchange (J = –35.0 cm^{-1}) has been reported

[a] *Ruđer Bošković Institute, Bijenička cesta 54, 10000 Zagreb, Croatia. E-mail: Marijana.Juric@irb.hr*
[b] *Department of Physics, Faculty of Science, University of Zagreb, Bijenička cesta 32, 10000 Zagreb, Croatia.*

† Electronic supplementary information (ESI) available: Powder X-ray diffraction patterns of **1** and **2** (Figs. S1 and S5), selected bond distances and angles for **1**–**3** (Table S1), molecular structures with the atom-numbering scheme of **1**–**3** (Fig. S2), hydrogen bonding patterns and geometry of **1**–**3** (Figs. S3, S6 and S7; Table S2), full interaction map of **1** (Fig. S4), aromatic stacking interactions of **3** (Fig. S8 and Table S3), intra and intermolecular distances for **1**–**3** (Table S4), χ(T) curve for **3** (Fig. S9) , DFT calculations details, structures, and polarization densities (Figs. S10–S12 and Table S6). Crystallographic data for **1**–**3** have been deposited with the Cambridge Crystallographic Data Centre as supplementary publication numbers CCDC 1580889–1580891. See DOI: 10.1039/x0xx00000x

Please do not adjust margins

for the compound in which copper(II) ions interact through triatomic –O–Zn–O– bridge, but the distance between these paramagnetic centres is significantly shorter (about 5.7 Å).[13]

In addition to the single-crystal and powder X-ray diffraction studies, IR spectroscopy and measurements on a SQUID magnetometer, the characterization of three novel oxo-bridged [$Cr^{III}Nb^{V}$] compounds have been accomplished by means of DFT calculations.

Results and discussion

Synthesis and crystal structure of compounds 1–3

From the reaction of aqueous solutions of tris(oxalato)oxoniobate(V) anions and bis(phenanthroline)chromium(III) cations in the molar ratio 1 : 1, heterometallic reddish crystalline compound $[Cr_2(phen)_4(\mu\text{-}O)_4Nb_2(C_2O_4)_4]\cdot 2H_2O$ (**1**) has been obtained (phen = 1,10-phenanthroline). The pink stick-like single crystals of **1**, of the quality needed for X-ray analysis, are obtained by slow liquid diffusion.[14] The Rietveld refinement confirmed that obtained reddish powder is single-phased polycrystalline sample of **1** (Fig. S1†). The crystal structure of compound **1** was used as a structural model for the Rietveld refinement on the powder data, and this procedure yielded a very satisfactory fit.

Compound **1** crystallizes in the tetragonal $P4_22_12$ space group consisting of targeted square $\{Cr_2(\mu\text{-}O)_4Nb_2\}$ core, in which Cr^{III} and Nb^{V} ions are alternately bridged by oxo ions (Figs. 1a and S2a†), and two water molecules of crystallization. Selected bond distances and angles are given in Table S1†. The chromium(III) ion displays a distorted octahedral coordination involving four N atoms from two coordinated phen ligands and two bridging oxygen atoms. Niobium(V) is coordinated by four O atoms from two bidentate oxalate groups and two bridging oxygen atoms. This octahedral coordination, $[NbO_2(C_2O_4)_2]^{3-}$, although reported in a similar coumpound,[6,7] is quite untypical since Nb^{V} usually displays pentagonal bipyramid coordination, $[NbO(C_2O_4)_3]^{3-}$, in known precursors.[15,16] The values of the Cr–O and Cr–N bond lengths are in good agreement with literature data,[6,7,17] as well those of the Nb–O and Nb–O_{ox}.[6,7]

The oxygen atoms from the oxalate groups of the square units and the crystallization water molecules, located on a twofold axis, participate in hydrogen bonding, resulting in 1D-arrangement parallel to the *c* axis (Fig. S3†, Table S2†). Full interaction map (Fig. S4†) of neutral but quite bulky molecule (wt = 1162.64 g mol^{-1}) points that the molecule has clearly divided hydrophobic (phen) from hydrophilic (oxalates) regions.

In an analogous molecule containing smaller bpy ligand,[6] molecules are more densely packed obviously due to steric reasons, with the shortest distance between their centres of gravity being 10.034 Å, compared to 12.198 Å in **1**. However, the molecules are arranged in higher symmetry in **1**, pointing out that phen ligand strengthens/stabilizes and fixes the core structure more effectively, probably due to its rigidness and superior chelating features.

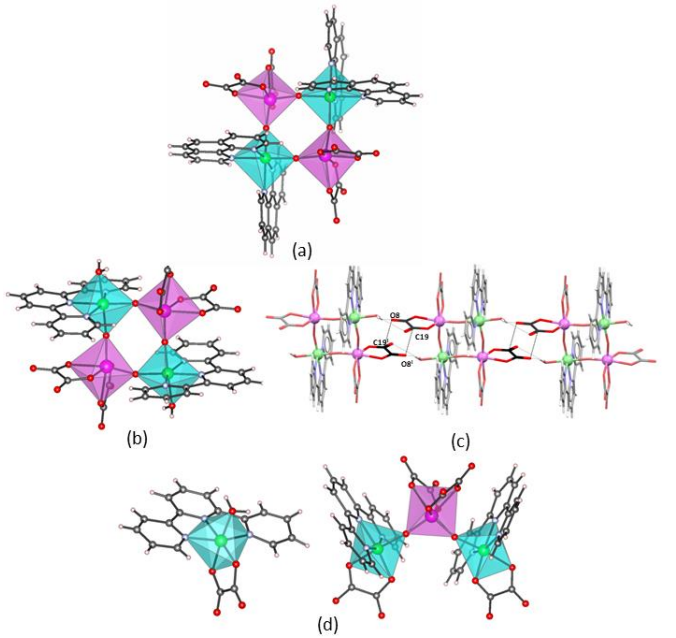

Fig. 1. (a) and (b) Heterotetranuclear $[Cr_2(L)_4(\mu\text{-}O)_4Nb_2(C_2O_4)_4]$ units in **1** (L = phen) and **2** (L = terpy), respectively. (c) Chains formed by stacking-like interactions between the antiparallel carbonyl groups in **2**. (d) A mononuclear $[Cr(terpy)(C_2O_4)(H_2O)]^{+}$ cation and heterotrinuclear $[Cr_2(terpy)_2(C_2O_4)_2(\mu\text{-}O)_2Nb(C_2O_4)_2]^{-}$ anion in **3**. The octahedra around the Cr and Nb atoms are depicted in light blue and violet colours, respectively.

Following a procedure similar to the one we have used for the preparation of **1**, but using tridentate 2,2′:6′,2′′-terpyridine (terpy) instead of bidentate phen ligand in complex cation of chromium(III), purple crystalline compound $[Cr_2(terpy)_2(H_2O)_2(\mu\text{-}O)_4Nb_2(C_2O_4)_4]\cdot 4H_2O$ (**2**) is isolated. Applying layering technique, the single crystals of **2** are obtained, and they crystallize in the $P2_1/n$ space group (Fig. S5†). The use of tridentate *N*-donor ligand also favours the formation of square shape $\{Cr_2(\mu\text{-}O)_4Nb_2\}$ core, with both metals adopting the octahedral geometry. Chromium ion is surrounded by three N atoms from a terpy molecule, two bridging oxo atoms and a coordinated water molecule in apical position (Figs. 1b and S2b†; Table S1†). Each square unit is interconnected with surrounding six molecules *via* direct hydrogen bonds coming from two hydrogen bond donors (coordinated water molecules) and two acceptors (two oxalate ligands), forming an overall 3D supramolecular architecture. Two crystallization water molecules present in asymmetric unit are also participating in hydrogen bonding assembly (Fig. S6†, SI, Table S2†).

An unusual intermolecular contact resembling π-stacking was noticed between oxalate moieties in the crystal packing of **2** (Fig. 1c). The oxalates planes are parallel and the interplanar distance is 2.930 Å; the interatomic distance between carbonyl oxygen O8 and carbon $C19^{i}$ is 2.992(4) Å (symmetry operator: (*i*) 2–*x*, –*y*, 1–*z*). This is one of the shortest C···O close contacts found in the Cambridge Structural Database (CSD)[18] and is considerably shorter than the sum of van der Waals radii (3.22 Å). It likely occurs due to electrostatic attraction of electron-rich carbonyl oxygen and severely electron-depleted carbon atom; antiparallel dipoles of carbonyl groups also contribute to

the total interaction. Similar contacts involving ketone- and carboxylate groups are well-known, however, similar contacts between oxalates are not very common (12 examples in CSD).[18] In these interactions mean planes of the oxalate moieties are almost perfectly normal; this is only the second example of parallel oxalates.[19] Each square unit forms two such oxalate···oxalate contacts, thus forming chains running in the direction of the axis *a*, together with hydrogen bonds (Fig. 1c).

In a period of 5 days, in the mother liquor, beside compound **2**, reddish prismatic crystals of complex salt $[Cr(terpy)(C_2O_4)(H_2O)][Cr_2(terpy)_2(C_2O_4)_2(\mu\text{-}O)_2Nb(C_2O_4)_2]\cdot 3H_2O$ (**3**), crystallizing in the triclinic $P\bar{1}$ space group, start to appear. The crystal structure consists of the mononuclear cations, $[Cr(terpy)(C_2O_4)(H_2O)]^+$, oxo-bridged heterotrinuclear anions, $[Cr_2(terpy)_2(C_2O_4)_2(\mu\text{-}O)_2Nb(C_2O_4)_2]^-$ (Figs. 1d and S2c†), and crystal water molecules. In this compound the square-shape geometry of the oxo-bridged metal centres is not observed, but rather a new type of trinuclear oxo-bridged anionic species consisting of two Cr^{III} and one Nb^{V} atom is formed. Additionally, ligand substitution is taking place prior to formation of **3**, in which complex cation $[Cr(terpy)(H_2O)_3]^{3+}$ present in the starting solution reacts with oxalate ligand to give $[Cr(terpy)(C_2O_4)(H_2O)]^+$ cation. The formation of this species is possible because starting Nb^{V} compound contains three coordinated oxalate groups and during transformation into a square-shaped complex one of the oxalate ligands is released from niobium sphere, providing free oxalate ligands in the reaction mixture. Since compound **3** is a complex salt, its solubility compared to neutral tetranuclear complex **2** is expected to be higher, explaining the subsequent crystallization. Similar square opening was not observed in systems with bpy and phen ligands, which can probably be attributed to steric reasons, i.e. more bulky terpy ligand. All metal centres in **3** have octahedral geometry; in the cation, Cr^{III} atom is coordinated by three N atoms from terpy molecule, two O atoms from bidentate oxalate group and one coordinated water, while in the anion instead of water molecule, bridging oxo atom is coordinated (Table S1†). The coordination polyhedron around Nb^{V} is similar to that ones in **1** and **2**.

Compared to **1** and **2**, in **3** various crystal packing motifs are observed. Hydrogen bonding network is complex, extending in all three dimensions. Each mononuclear cation forms direct hydrogen bond with two surrounding trinuclear anions, and one crystallization water molecule is mediating additional hydrogen bond between cation and anion (Fig. S7†, Table S2†). Stacking interactions are interconnecting a pair of anions and each anion is additionally stacked with one cation, forming discrete π-stacked tetramers along the [111] direction (Fig. S8†, Table S3†).

Infrared study

An infrared spectrum of **1** confirmed the presence of the oxygen bridges: the maximum at 870 cm^{-1} of strong and broad absorption band corresponding to the Cr–O–Nb asymmetric stretching vibration (the Cr–O–Nb angle is 170.4°; Table S1†) was observed.[6,20] The strong absorption band with maximum at 872 cm^{-1} in spectrum of **2** is also indicative of the oxo bridge vibrations.[20] The values of the Cr–O–Nb angles in **2** are more similar (164.73 and 167.60°; Table S1†) than in **3**, where the difference between these angles is larger (156.80 and 163.81°; Table S1†); so in the IR spectrum of **3** there are two resolved absorption bands corresponding to the ν(M–O–M) stretching vibration, with maxima at 828 and 873 cm^{-1}.[20]

Other absorption bands of the significant intensity in the spectra **1**–**3** correspond to different vibrations of chelating bidentate oxalate groups and coordinated *N*-donor ligands.[20]

Magnetization study

The temperature dependences of the molar magnetic susceptibility, $\chi(T)$, for compounds **1**–**3** are shown in Fig. 2.

For **1** and **2**, molar magnetic susceptibility upon cooling rises to the local maximum value around 15 K, after which it decreases, suggesting antiferromagnetic ground state. After the local minimum, $\chi(T)$ rises upon further cooling in the way characteristic for the small paramagnetic impurity contribution.[13]

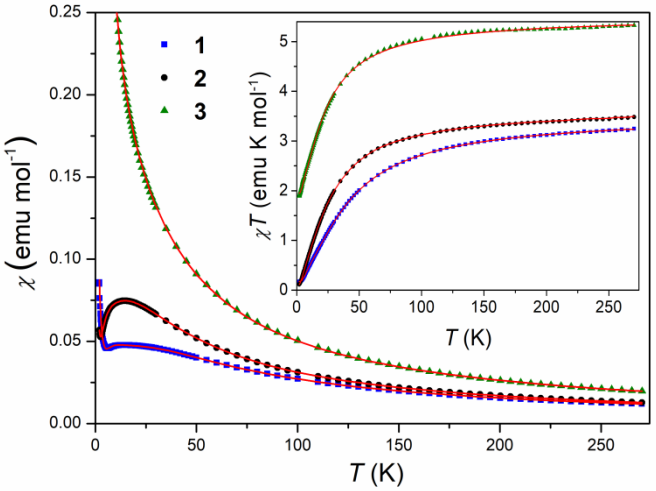

Fig. 2 Temperature dependence of molar magnetic susceptibility χ for compounds **1**–**3**. Inset: Temperature dependence of the product χT. The solid lines represent the best-fitted model curves.

Based on the crystal structure and known example,[6] magnetic data for **1** and **2** are modelled using Hamiltonian:

$$H = -J\boldsymbol{S}_1 \cdot \boldsymbol{S}_2 + \sum_{i=1}^{2} D\left(S_{z,i}^2 - \frac{S(S+1)}{3}\right) + 2g\mu_B \boldsymbol{S}_i \cdot \boldsymbol{B} \qquad (1)$$

where J is parameter of the magnetic interaction between Cr^{III} ions through diamagnetic –O–Nb^{V}–O– bridge, D is single ion axial zero-field splitting parameter, g and μ_B have usual meaning. As it is evident from the $\chi(T)$ curves of compounds **1** and **2**, certain amount of paramagnetic impurity is present, and therefore paramagnetic contribution is added to the magnetic contribution coming from the Hamiltonian (eq. 1). The exact nature of that impurity is not known, but in fit it is assumed that comes from two paramagnetic chromium(III) centres. Also, the square units in both compounds are quite

distant from each other (Table S4†), and there is no intermolecular coupling between chromium(III) ions.

The experimental data for **3** shows an increase of the $\chi(T)$, and a decrease of $\chi T(T)$ values (the inset of Fig. 2) by cooling. Dropping of the $\chi T(T)$ suggests antiferromagnetic coupling between two chromium ions in $[Cr_2(terpy)_2(C_2O_4)_2(\mu\text{-}O)_2Nb(C_2O_4)_2]^-$, with the value of 1.88 emu K mol^{-1} at 2 K, corresponding to the contribution of Cr^{III} with spin S = 3/2. Large growth of χ in the low temperature region comes from paramagnetic behaviour of Cr^{III} from $[Cr(terpy)(C_2O_4)(H_2O)]^+$. The temperature dependence of χ in full range for this compound is shown in Fig. S9†. Compound **3** consists of three chromium ions per formula unit (one from mononuclear cation and two from trinuclear anion). There is no magnetic interaction between chromium(III) atoms from the cation and anion; they are far from each other (Table S4† and DFT calculations). Its magnetic behaviour is therefore modelled using Hamiltonian:

$$H = -J\boldsymbol{S}_1 \cdot \boldsymbol{S}_2 + \sum_{i=1}^{3} D\left(S_{z,i}^2 - \frac{S(S+1)}{3}\right) + 3g\mu_B \boldsymbol{S} \cdot \boldsymbol{B} \qquad (2)$$

The best fit parameters for all compounds are shown in the Table 1.

Antiferromagnetic behaviour of two chromium(III) ions through diamagnetic bridge is observed in all compounds (Table 1); **1** exhibits somewhat stronger interaction (J = –13.51 cm^{-1}) than **2** and **3** (J = –8.41 and –7.44 cm^{-1}, respectively). Obviously, the structural features have an effect on the smaller J in **2** and **3.** It is known that linearity of the oxo bridges influences the most strength of magnetic interaction. Compound **1** has the least bent geometry (value of Cr–O–Nb angle is 170.4°; Table S1†) and interaction is the strongest, while for compounds **2** and **3** same corresponding angles are 166.17° and 160.31° in averages, respectively (Table S1†), and strength of the coupling interactions decreases in that order (Table 1).

Table 1 The best fit parameters for compounds **1**–**3** as well as magnetic exchange parameters J obtained with GGA+U DFT calculation

Comp.	g	J / cm^{-1}	|D| / cm^{-1}	ρ / %[a]	J_{DFT} / cm^{-1}
1	1.98	–13.51	0.23	4.91	–9.88
2	1.98	–8.41	0.11	2.93	–11.41
3	1.98	–7.44	0.10	–	–9.91

[a] the fraction of the paramagnetic impurity.

DFT calculations

To support these investigations and give further atomistic understanding, density functional theory (DFT) calculations of compounds **1**–**3** are performed. As shown in Fig. S10† optimised geometries calculated with PBE,[21] GGA+U,[22] and vdW-DF-cx[23] functionals are almost identical showing that it is not important to include vdW forces for these compounds (see DFT calculations in Experimental). In all cases DFT predicts antiferromagnetic ground state and each Cr atom carries spin S = 3/2 in accordance with other experimental results. Figs. S11† and S12† show spin polarization density calculated with the three DFT functionals for compound **1** (the same density distributions are obtained also for **2** and **3**). As expected (see DFT calculations in Experimental), GGA+U shows better spin localization around Cr atoms compared to PBE and vdW-DF-cx, as can be seen for low densities in Fig. S11† (at higher densities there are no differences, Fig. S12†). Considering only GGA+U (Fig. 3) it can be seen that oxygen atoms, depending on the polarization of a surrounding chromium atoms, have an opposite spin polarization – a screening effect. Niobium atoms have a very small, but not negligible polarization density (Fig. 3). The J parameters obtained with GGA+U DFT calculation are listed in Table 1. DFT predicts similar J values as the fitting procedure, confirming applicability of above model (eq.1 and 2), though, the largest J is obtained for **2**. Other two functionals (that suffer from delocalization error) predict larger spin polarization on Nb atoms and larger J as shown in Table S6†, containing magnetic and structural properties calculated with the three DFT functionals. Since there are two isolated molecules per unit cell in **1** and **2**, and two cations and two anions in **3**, magnetic interaction between them can be also estimated by setting different magnetic configurations. We obtained no difference in energy up to our precision, which means that magnetic intermolecular interaction is at least two orders of magnitude smaller than intramolecular interaction via bridge.

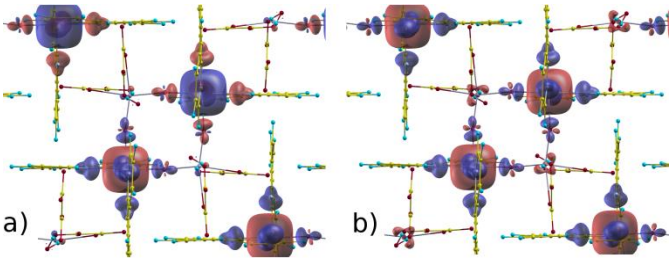

Fig. 3 Magnetic polarization density (difference of spin up and spin down electron density) for compound **1** obtained with GGA+U: (a) antiferromagnetic solution, (b) ferromagnetic solution. Isosurface value is 0.003 electrons/a.u.^{3}.

Conclusions

We have shown that $[NbO(C_2O_4)_3]^{3-}$ is very effective building block for multitopic binding to metal centres. In reactions with chromium(III) precursor, regardless of the ancillary *N*-donor ligand used to chelate Cr^{III}, oxo-bridged complexes are formed with six-coordinated Nb^V. Triatomic diamagnetic –O–Nb^V–O– bridge either from tetra- (square) in **1** and **2**, or trinuclear units (square opening) in **3** transmit antiferromagnetic exchange interaction between Cr^{III} ions. Probably, due to steric reasons i.e. bulkier terpy ligand, the square unit containing two –O–Nb^V–O– bridges is "broken", leading to the formation of trinuclear unit with only one bridge. Probably, due to steric reasons i.e. bulkier terpy ligand, the square unit containing two –O–Nb^V–O– bridges is "broken", leading to the formation of trinuclear compound with only one —O–Nb^V–O– bridge.

Experimental and calculated studies, which are in good agreement, have shown that a square core is not important for the occurrence and strength of antiferromagnetic interaction through diamagnetic –O–Nb^V–O– bridge, whereas linearity of the bridge is an important factor.

Our further research would be related to the synthesis and characterization of (similar) oxo-bridged compounds prepared from tris(oxalato)oxoniobate(V), $[NbO(C_2O_4)_3]^{3-}$ anions and precursor containing other paramagnetic cation, such as vanadium or rhodium, in order to explore unique and unconventional magnetic interaction through diamagnetic O–Nb^V–O– bridges in other transition metal complexes.

Experimental

Materials and physical measurements

The chemicals were purchased from commercial sources and used without further purification. The starting species $(NH_4)_3[NbO(C_2O_4)_3]\cdot H_2O$ and chromium(III) precursor solution were prepared following a specific procedure described previously.[6,24] Elemental analyses for C, H and N were performed with a Perkin–Elmer Model 2400 microanalytical analyzer. The infrared spectra were recorded in the 4000–350 cm^{-1} region with samples as KBr pellets, with a Bruker Alpha FTIR spectrometer.

Synthetic procedures

Synthesis of $[Cr_2(phen)_4(\mu\text{-}O)_4Nb_2(C_2O_4)_4]\cdot 2H_2O$ (1). An aqueous solution (15 mL) of $(NH_4)_3[NbO(C_2O_4)_3]\cdot H_2O$ (178.0 mg, 0.4 mmol) was added with a dropper to an aqueous solution (8 mL) of chromium precursor complex [*n*(Cr) = 0.4 mmol; *n*(phen) = 0.8 mmol]. The reaction mixture was stirred at room temperature for a short period of time. The reddish crystalline powder of **1** appeared very quickly. The precipitate was separated from the solution by filtration, washed with water, and left to dry in air. The yield was 58.20%. Anal. Calcd for $C_{56}H_{36}Cr_2N_8Nb_2O_{22}$ (**1**): C, 45.98; H, 2.48; N, 7.66: Found: C, 45.92; H, 2.51; N, 7.63. IR data (KBr, cm^{-1}): 1718 (s), 1705 (vs) and 1677 (s) [ν_{as}(CO)], 1353 (s) and 1220 (m) [vs(CO)], 787 (m) [δ(OCO)], 870 (vs) [ν_{as}(CrONb)].[6,20]

Single crystal growth of 1. A mixture of an aqueous solution (2 mL) of chromium precursor complex [*n*(Cr) = 0.1 mmol; *n*(phen) = 0.2 mmol] and acetonitrile (8 mL) was carefully laid above an aqueous solution (5 mL) of $(NH_4)_3[NbO(C_2O_4)_3]\cdot H_2O$ (44.51 mg; 0.1 mmol) into a test tube. The X-ray quality pink stick-like crystals of **1** were formed after two days.

Synthesis of $[Cr_2(terpy)_2(H_2O)_2(\mu\text{-}O)_4Nb_2(C_2O_4)_4]\cdot 4H_2O$ (2) and $[Cr(terpy)(C_2O_4)(H_2O)][Cr_2(terpy)_2(C_2O_4)_2(\mu\text{-}O)_2Nb(C_2O_4)_2]\cdot 3H_2O$ (3). To an aqueous solution (10 mL) containing $(NH_4)_3[NbO(C_2O_4)_3]\cdot H_2O$ (44.51 mg, 0.1 mmol), an aqueous solution (2 mL) of chromium precursor complex [*n*(Cr) = 0.1 mmol; *n*(terpy) = 0.1 mmol] was added. After three days, from the resulting clear reddish solution, the purple crystalline powder of **2** started to appear. Within a period of 5 days, from the mother-liquid reddish prismatic crystals, identified as compound **3**, started to grow. The crystals were separated from the solution, washed with water, and left to dry in air. The yield was 42.30%. Anal. Calcd for $C_{38}H_{34}Cr_2N_6Nb_2O_{26}$ (**2**): C, 35.64; H, 2.68; N, 6.56: Found: C, 35.69; H, 2.65; N, 6.51. IR data of **2** (KBr, cm^{-1}): 1722 (vs), 1704 (vs), 1682 (vs) and 1665 (s) [vas(CO)], 1369 (s) and 1230 (m) [vs(CO)], 796 (m) [δ(OCO)], 872 (vs) [vas(CrONb)].[6,20] Anal. Calcd for $C_{55}H_{41}Cr_3N_9NbO_{26}$ (**3**): C, 44.25; H, 2.77; N, 8.45: Found: C, 44.30; H, 2.79; N, 8.43. IR data of 3 (KBr, cm^{-1}): 1715 (vs) and 1686 (s) [vas(CO)], 1356 (s) and 1221 (m) [vs(CO)], 801 (m) [δ(OCO)], 873 (m) and 828 (s) [ν_{as}(CrONb)].[6,20]

Single crystal growth of 2. An aqueous solution (5 mL) of $(NH_4)_3[NbO(C_2O_4)_3]\cdot H_2O$ (22.25 mg; 0.05 mmol) was layered with a mixture of an aqueous solution (3 mL) of chromium precursor complex [*n*(Cr) = 0.15 mmol; *n*(terpy) = 0.15 mmol] and 7 ml of acetonitrile, in a test tube. Reddish prismatic crystals of **2** were formed after seven days.

Single-crystal X-ray structural study

The X-ray data for single crystal of compound **1** was collected at 293(2) K by ω-scans on an Oxford Diffraction Xcalibur Nova R diffractometer with the graphite monochromated Cu-Kα radiation (λ = 1.54179 Å, microfocus tube, CCD detector). Crystals of **2** and **3** were measured on D8 Venture Bruker diffractometer with dual microsource Ag-Mo radiation (using Mo-Kα radiation, λ = 0.71073 Å, CCD detector) at 100(2) and 293(2) K, respectively. Crystal data and details of data collections and refinements for the structures reported are summarized in Table 2. Data reduction, including the multi-scan absorption correction, was performed with the CrysAlisPRO software[25] package for compound **1**, and with the SAINT software[26] package for compounds **2** and **3**. Solution, refinement and analysis of the structures were performed using the programs integrated in the WinGX system.[27] The structures were solved by direct methods (SIR92)[28] and refined by the full-matrix least-squares method based on F2 against all reflections (SHELXL-2017/1).[29] The hydrogen atoms attached to carbon atoms of aromatic ligands were treated as riding in idealized positions, with the C–H distances of 0.93 Å and displacement parameters assigned as U_{iso}(H) = 1.2U_{eq}(C). The geometry of water molecule was restrained to the target values [O–H distance of 0.85(2) Å and H–O–H angles of 104°. Geometrical calculations were carried out with PLATON[30] and the figures were made by the use of the ORTEP,[27] CCDC-Mercury[31] and VESTA[32] programs.

Powder X-ray structural study

The powder XRD patterns were measured in the reflection mode with monochromated Cu-Kα radiation (λ = 1.54179 Å) with a Philips PW1830 diffractometer. The Rietveld refinement was performed by the HighScore X'pert Plus program (Panalytical) and Topas Academic. On the basis of the choice of structural mode and the type of profile function, the program simulates the XRD patterns and compares them with the experimental ones in the least-square comparison mode. Thus, a certain number of least-squares structural and profile parameters were refined. The diffraction profiles were described by the pseudo Voigt function. A polynomial model was used to describe the background. Five background parameters, a scale factor, a zero-point shift, half-width parameters (*U*, *V*, *W*), peak-shape parameters and asymmetry parameters were included in the refinement. The structural parameters, atomic coordinates and B_{iso} were also refined.

Magnetization study

The magnetization *M* of compounds **1**–**3** in powder form was measured with a MPMS 5 commercial superconducting quantum interferometer device (SQUID) magnetometer. The measured magnetic moments of the samples were corrected against the sample holder contribution and the temperature-independent contributions of the core electrons in accordance with the well-known Pascal formula. The temperature dependence of magnetization for all compounds, $M(T)$, was measured in the temperature range 2–270 K.

DFT calculations

The plane-wave DFT code Quantum ESPRESSO[33] with GBRV pseudopotentials[34] was used to study magnetic and structural properties of the compounds **1**–**3**. The energy cut-off for the plane wave basis set is set to 680 eV. Relaxation of ionic positions starting from experimental structures was performed until forces on all atoms were smaller than 0.01 eV $Å^{-1}$ and change in energy of two consecutive steps was smaller than 0.5 meV. Positions of hydrogens in water were not resolved for compounds **1** and **3** so they were added by hand before relaxation. The Brillouin zone is sampled with a 2×2×2 Monkhorst-Pack mesh. We use three exchange-correlation functional, standard PBE,[21] GGA+U approach[22] to better describe localized d-electrons (with GGA = PBE), and vdW-DF-cx[23] to check influence of van der Waals forces which are mostly neglected in other two. Parameter *U* is set to value of 3.5 eV, as it was shown that this value reproduces much more expensive hybrid functional calculations.[6] Exchange parameters *J* are calculated from differences of total energies of unit cell for ferromagnetic (E_{FM}) and antiferromagnetic state (E_{AFM}), $\Delta E = E_{AFM} - E_{FM}$. Since in each compound there are two pairs of bridged Cr atoms and each Cr atom has spin 3/2, the exchange constant is calculated as $J = \Delta E / 9$.

Acknowledgements

This work has been supported by the Croatian Science Foundation under Project Nos. IP-2014-09-4079 and UIP-2014-09-8276. I. L. was supported by the Unity Through Knowledge Fund, Contract No. 22/15 and H2020 CSA Twinning Project No. 692194, RBI-T-WINNING.

Notes and references

1 a) M. Nihei, Y. Yanai, I.-J. Hsu, Y. Sekine and H. Oshio, *Angew. Chem. Int. Ed.*, 2016, **55**, 1–5; b) E. Coronado, J. R. Galán-Mascarós and C. Martí-Gastaldo, *J. Am. Chem. Soc.,* 2008, **130**, 14987–14989; c) E. Coronado, C. Martí-Gastaldo, J. R. GalánMascarós and M. Cavallini, *J. Am. Chem. Soc.,* 2010, **132**, 5456–5468; d) X.-Y. Wang, C. Avendañoand Kim R. Dunbar, Chem. Soc. Rev., 2011, **40**, 3213–3238. e) J. Mroziński, *Coord. Chem. Rev.*, 2005, **249**, 2534–2548.

2 a) C. Maxim, S. Ferlay, H. Tokoro, S.-I. Ohkoshi and C. Train, *Chem. Commun.*, 2014, **50**, 5629–5632; b) E. Pardo, C. Train, H. Liu, L.-M. Chamoreau, B. Dkhil, K. Boubekeur, F. Lloret, K. Nakatani, H. Tokoro, S.-i. Ohkoshi and M.Verdaguer, *Angew. Chem. Int. Ed.*, 2012, **51**, 8356–8360; c) E. Pardo, C. Train, G. Gontard, K. Boubekeur, O. Fabelo, H. Liu, B. Dkhil, F. Lloret, K. Nakagawa, H. Tokoro, S.-i. Ohkoshi and M. Verdaguer, *J. Am. Chem. Soc.,* 2011, **133**, 15328–15331; d) D. Masposh, D. Ruiz-Molina and J. Veciana, *Chem. Soc. Rev.*, 2007, **36**, 770–818.

3 B. Sieklucka, P. Dawid, (Editors) *Molecular Magnetic Materials: Concepts and Applications*, Wiley-VCH, Verlag GmbH & Co. KgaA, 2017.

4 M. Jurić, B. Perić, N. Brničević, P. Planinić, D. Pajić, K. Zadro and G. Giester, *Polyhedron*, 2007, **26**, 659–672.

5 M. Jurić, P. Planinić, N. Brničević, D. Matković-Čalogović, J. Mol. Struct. 2008, **888**, 266–276.

6 M. Jurić, L. Androš Dubraja, D. Pajić, F. Torić, A. Zorko, A. Ozarowski, V. Despoja, W. Lafargue-Dit-Hauret and X. Rocquefelte, *Inorg. Chem.*, 2017, **56**, 6879–6889.

7 W. X. C. Oliveira, C. L. M. Pereira, C. B. Pinheiro, J. Cano, F. Lloret and M. Julve, *Chem. Commun.*, 2015, **51**, 11806–11809.

8 Y. Journaux, J. Sletten and O. Kahn, *Inorg. Chem.*, 1986, **25**, 439–447.

9 P. Chaudhuri, M. Winter, K. Wieghardt, S. Gehring, W. Haase, B. Nuber and J. Weiss, *Inorg. Chem.*, 1988, **27**, 1564–1569.

10 P. Chaudhuri, M. Winter, B. P. C. Della Védova, E. Bill, A. Trautwein, S. Gehring, P. Fleischhauer, B. Nuber and J. Weiss, *Inorg. Chem.*, 1991, **30**, 2148–2157.

11 H. Oshio, T. Kikuchi and T. Ito, *Inorg. Chem.*, 1996, **35**, 4938–4941.

12 R. Ruiz, M. Julve, J. Faus, F. Lloret, M. Carmen Muñoz, Y. Journaux and C. Bois, *Inorg. Chem.*, 1997, **36**, 3434–3439.

13 E. A. Buvaylo, V. N. Kokozay, O. Yu. Vassilyeva, B. W. Skelton, J. Jezierska, L. C. Brunel and A. Ozarowski, *Chem. Commun.*, 2005, 4976–4978.

14 B. Spingler, S. Schnidrig, T. Todorova and F. Wild, *CrystEngComm*, 2012, **14**, 751–757.

15 M. Šestan, B. Perić, G. Giester, P. Planinić, N. Brničević, *Struct. Chem.*, 2005, **16,** 409–414.

16 M. Jurić, B. Perić, N. Brničević, P. Planinić, D. Pajić, K. Zadro, G. Giester and B. Kaitner, *Dalton Trans.*, 2008**,** 742–754.

17 L. Androš, M. Jurić, K. Molčanov and P. Planinić, *Dalton Trans.*, 2012, **41**, 14611–14624.

18 C. R. Groom, I. J. Bruno, M. P. Lightfoot and S. C. Ward, *Acta Crystallogr., Sect. B: Struct. Sci., Cryst. Eng. Mater.*, 2016, **B72**, 171–179.

19 N. Casati, P. Macchi and A. Sironi, *Chem. Commun*., 2009, 2679–2681.

20 K. Nakamoto, *Infrared and Raman Spectra of Inorganic and Coordination Compounds*, John Wiley, New York, 6th edn, 2009.

21 J. P. Perdew, K. Burke and M. Ernzerhof, *Phys. Rev. Lett.*, 1996, **77**, 3865.

22 M. Cococcioni and S. de Gironcoli, *Phys. Rev. B*, 2005, **71**, 035105.

23 K. Berland and P. Hyldgaard, *Phys. Rev. B*, 2014, **89**, 035412.

24 M. Jurić, J. Popović, A. Šantić, K. Molčanov, N. Brničević and P. Planinić, *Inorg. Chem.*, 2013, **52**, 1832–1842.

25 Agilent. CrysAlis PRO; Agilent Technologies Ltd: Yarnton, England, 2014.

26 Bruker, *SAINT V8.34A*, Bruker AXS Inc., Madison, WI, 2013.

27 L. J. Farrugia, *J. Appl. Crystallogr*., 2012, **45**, 849–854.

28 A. Altomare, G. Cascarano, C. Giacovazzo, A. Guagliardi, M. C. Burla, G. Polidori and M. Camalli, *J. Appl. Crystallogr*. **1994**, *27*, 435.

29 G. M. Sheldrick, *Acta Crystallogr., Sect. A: Cryst. Phys., Diffr., Theor. Gen. Cryst.*, 2015, **71**, 3–8.

30 A. L. Spek, *Acta Crystallogr., Sect. D: Biol. Crystallogr.*, 2009, **65**, 148–155.

31 C. F. Macrae, P. R. Edgington, P. McCabe, E. Pidcock, G. P. Shields, R. Taylor, M. Towler and J. van de Streek, *J. Appl. Crystallogr.*, 2006, **39**, 453–457.

32 K. Momma and F. Izumi, *J. Appl. Crystallogr.*, 2011, **44**, 1272–1276.
33 P. Giannozzi, S. Baroni, N. Bonini, M. Calandra, R. Car, C. Cavazzoni, D. Ceresoli, G. L. Chiarotti, M. Cococcioni, I. Dabo, A. Dal Corso, S. de Gironcoli, S. Fabris, G. Fratesi, R. Gebauer, U. Gerstmann, C. Gougoussis, A. Kokalj, M. Lazzeri, L. Martin-Samos, N. Marzari, F. Mauri, R. Mazzarello, S. Paolini, A. Pasquarello, L. Paulatto, C. Sbraccia, S. Scandolo, G. Sclauzero, A. P. Seitsonen, A. Smogunov, P. Umari and R. M. Wentzcovitch, *J. Phys.: Condens. Matter*, 2009, **21**, 395502.
34 K. F. Garrity, J. W. Bennett, K. M. Rabe and D. Vanderbilt, *Comput. Mater. Sci.*, 2014, **81**, 446.

Table 2 Crystallographic data and structure refinement details for compounds $[Cr_2(phen)_4(\mu\text{-}O)_4Nb_2(C_2O_4)_4]\cdot 2H_2O$ (**1**), $[Cr_2(terpy)_2(H_2O)_2(\mu\text{-}O)_4Nb_2(C_2O_4)_4]\cdot 4H_2O$ (**2**) and $[Cr(terpy)(C_2O_4)(H_2O)][Cr_2(terpy)_2(C_2O_4)_2(\mu\text{-}O)_2Nb(C_2O_4)_2]\cdot 3H_2O$ (**3**)

compound	**1**	**2**	**3**
T (K)	293(2) K	100(2)	293(2) K
Crystal colour, habit	pink, needle	red, stick	pink, needle
Empirical formula	$C_{56}H_{34}Cr_2N_8Nb_2O_{22}$	$C_{38}H_{34}Cr_2N_6Nb_2O_{26}$	$C_{55}H_{41}Cr_3N_9Nb_1O_{26}$
Formula wt/g mol^{-1}	1460.72	1280.54	1492.88
Crystal system	tetragonal	monoclinic	triclinic
space group	$P4_22_12$	$P2_1/n$	$P\bar{1}$
a/Å	14.770(5)	11.0343(9)	14.206(5)
b/Å	14.770(5)	17.4862(14)	14.903(5)
c/Å	12.583(5)	11.9713(7)	15.710(5)
α/°	90	90	71.440(5)
β/°	90	90.766(3)	88.232(5)
γ/°	90	90	68.059(5)
V/Å^3	2745.0(2)	2309.6(3)	2909.9(17)
Z	8	4	2
ρ_c/g cm^{-3}	1.767	1.841	1.704
μ/mm^{-1}	7.310	1.043	6.916
F(000)	1464	1284	1510
Crystal size/mm^3	0.39×0.06×0.06	0.269×0.075×0.069	0.257×0.106×0.059
Θ range/°	4.23−75.64	2.329−27.547	1.971-26.639
Reflections collected	15115	51049	131815
Independent reflections	2846	5310	11695
Observed reflections	2032	4154	8959
No. of parameters, restraints	209, 1	358, 9	853, 3
R_{int}	0.0688	0.1147	0.0634
R, wR [I > 2σ(I)]	0.0658, 0.1729	0.0376, 0.0766	0.0984, 0.2303
R, wR [all data]	0.0945, 0.1891	0.0602, 0.0844	0.1101, 0.2608
goodness-of-fit, S	1.108	1.059	0.923
$\Delta\rho_{max}$, $\Delta\rho_{min}$ (e Å^{-3})	2.014, −0.430	0.569, −0.78	0.599, −0.669